Published in final edited form as:
*Science*. 2010 November 26; 330(6008): 1247–1251. doi:10.1126/science.1189157.

# PML Regulates Apoptosis at Endoplasmic Reticulum by Modulating Calcium Release

**Carlotta Giorgi**[1,2,3,4], **Keisuke Ito**[3,4], **Hui-Kuan Lin**[4], **Clara Santangelo**[5], **Mariusz R. Wieckowski**[6], **Magdalena Lebiedzinska**[6], **Angela Bononi**[1], **Massimo Bonora**[1], **Jerzy Duszynski**[6], **Rosa Bernardi**[3,4,7], **Rosario Rizzuto**[8], **Carlo Tacchetti**[5,9], **Paolo Pinton**[1,3,4,*], and **Pier Paolo Pandolfi**[3,4,*]

[1]Department of Experimental and Diagnostic Medicine, Section of General Pathology, Interdisciplinary Center for the Study of Inflammation (ICSI), Emilia Romagna Laboratory BioPharmaNet, and Laboratory for Technologies of Advanced Therapies (LTTA) University of Ferrara, Ferrara, Italy. [2]Vita-Salute San Raffaele University, Center of Excellence in Cell Development, and IIT Network, Research Unit of Molecular Neuroscience, Milan, Italy. [3]Cancer Genetics Program, Beth Israel Deaconess Cancer Center, Departments of Medicine and Pathology, Beth Israel Deaconess Medical Center, Harvard Medical School, Boston, MA 02215, USA. [4]Cancer Biology and Genetics Program, Department of Pathology, Memorial Sloan-Kettering Cancer Center, New York, NY 10065, USA. [5]IFOM (FIRC Institute of Molecular Oncology Foundation) Centre of Cell Oncology and Ultrastructure MicroSCoBiO Research Center, Department of Experimental Medicine, University of Genova, Genova, Italy. [6]Nencki Institute of Experimental Biology, Warsaw, Poland. [7]San Raffaele Research Institute, Department of Molecular Oncology, Milan, Italy. [8]Department of Biomedical Sciences, University of Padua, Padua, Italy. [9]Scientific Institute San Raffaele, Experimental Imaging Center, Milan, Italy.

## Abstract

The promyelocytic leukemia (PML) tumor suppressor is a pleiotropic modulator of apoptosis. However, the molecular basis for such a diverse proapoptotic role is currently unknown. We show that extranuclear Pml was specifically enriched at the endoplasmic reticulum (ER) and at the mitochondria-associated membranes, signaling domains involved in ER-to-mitochondria calcium ion ($Ca^{2+}$) transport and in induction of apoptosis. We found Pml in complexes of large molecular size with the inositol 1,4,5-trisphosphate receptor ($IP_3R$), protein kinase Akt, and protein phosphatase 2a (PP2a). Pml was essential for Akt- and PP2a-dependent modulation of $IP_3R$ phosphorylation and in turn for $IP_3R$-mediated $Ca^{2+}$ release from ER. Our findings provide a mechanistic explanation for the pleiotropic role of Pml in apoptosis and identify a pharmacological target for the modulation of $Ca^{2+}$ signals.

The promyelocytic leukemia gene (*PML*)was originally identified at the breakpoint of the t(15;17) translocation of acute promyelocytic leukemia (APL), and function of the PML protein is frequently lost or aberrant in human solid tumors and hematopoietic malignancies



*To whom correspondence should be addressed. ppandolf@bidmc.harvard.edu (P.P.P.); pnp@unife.it (P.P.).

**Supporting Online Material**
www.sciencemag.org/cgi/content/full/science.1189157/DC1
Materials and Methods
Figs. S1 to S20
References

(1,2). PML is a nuclear protein and an essential component of subnuclear structures termed nuclear bodies (NBs) (3). However, many, if not all, PML isoforms have shown both cytoplasmic and nuclear localization (4,5). *Pml*$^{-/-}$ mice and primary cells are protected from apoptosis triggered by a number of diverse stimuli (6).

To determine how PML could regulate such broadly diverse apoptotic responses, we analyzed its intracellular localization by cell fractionation (7,8). We fractionated homogenates of primary mouse embryonic fibroblasts (MEFs) by ultracentrifugation, focusing on the mitochondria, endoplasmic reticulum (ER), and mitochondria-associated membranes (MAMs), the structures that contain sites where the ER contacts mitochondria. Pml localized both to the nucleus and the cytosol and appeared to localize also to the ER, MAM, and crude mitochondrial fractions but not to "pure" mitochondrial fraction free of ER and nuclear markers (Fig. 1A). These results were confirmed by immunogold labeling of ultrathin cryosections showing that Pml associates with the surface of the ER (Fig. 1B, a and b) and in the proximity of the mitochondrial membrane at contact sites between the ER and mitochondria (Fig. 1B, d to g).

In view of the localization of Pml at the ER and MAM, we investigated its requirement in apoptosis induced by ER stress (9). Matched wild-type (*Pml*$^{+/+}$) and *Pml*$^{-/-}$ MEFs were treated with ER stress inducers: $H_2O_2$ and menadione (MEN), two oxidizing agents that induce ER $Ca^{2+}$ release; tunicamycin (TN) or an inhibitor of protein N-glycosylation; and thapsigargin (TG), an inhibitor of the sarcoplasmic/ER $Ca^{2+}$-ATPase (adenosine triphosphatase). After 12 hours of treatment, the percentage of apoptotic cells in *Pml*$^{-/-}$ MEFs was much lower than that observed in *Pml*$^{+/+}$ MEFs under all treatment conditions (Fig. 1C and fig. S1).

MAMs are specialized domains selectively enriched in critical $Ca^{2+}$ signaling elements, which mediate $Ca^{2+}$ transfer between ER and mitochondria (10,11), such as the inositol 1,4,5-trisphosphate receptor ($IP_3R$) (12). $Ca^{2+}$ signaling has a major role in the regulation of cell death (13,14). Release of the ER $Ca^{2+}$ pool through the type 3 $IP_3R$ ($IP_3R3$) appears to induce a sensitization of cells to apoptotic stimuli (15,16).

To investigate the role of Pml in $Ca^{2+}$ homeostasis, we used recombinant $Ca^{2+}$-sensitive bioluminescent protein aequorin (17). In *Pml*$^{+/+}$ MEFs, the $Ca^{2+}$ concentration ($[Ca^{2+}]$) in the lumen of the ER ($[Ca^{2+}]_{ER}$) at steady state was ~450 μM, whereas in *Pml*$^{-/-}$ MEFs it was lower. When the cells were stimulated with adenosine 5′-triphosphate (ATP), the P2Y receptor agonist that causes release of $Ca^{2+}$ from the ER, the decreases in the $[Ca^{2+}]_{ER}$ observed in *Pml*$^{+/+}$ MEFs in quantitative and kinetic terms were larger and faster than in *Pml*$^{-/-}$ MEFs, reflecting a more rapid flow of $Ca^{2+}$ through the $IP_3R$ (Fig. 2A). In turn, the $[Ca^{2+}]$ increases evoked by stimulation with ATP in the cytosol ($[Ca^{2+}]_c$) and mitochondria ($[Ca^{2+}]_m$) were smaller in *Pml*$^{-/-}$ than in *Pml*$^{+/+}$ MEFs (Fig. 2, B and C, and fig. S2). A mitochondrial $Ca^{2+}$ deregulation was observed also in human-derived cells in which PML was depleted (fig. S3) and in different cellular models of APL (fig. S4).

We then investigated whether the absence of Pml could alter the increases in $[Ca^{2+}]_c$ and $[Ca^{2+}]_m$ induced by apoptotic stimuli. In *Pml*$^{-/-}$ MEFs, the increases in $[Ca^{2+}]_c$ and $[Ca^{2+}]_m$, evoked by the oxidative apoptotic stimuli, such as MEN and $H_2O_2$ that trigger both a progressive release of $Ca^{2+}$ from the ER and an activation of the capacitative $Ca^{2+}$ influx (18), were smaller as mentioned above (Fig. 2, D and E).

To determine whether the effects of Pml on regulation of $Ca^{2+}$ homeostasis depend on its localization to the ER and MAMs, we generated a chimeric protein containing the entire PML protein that was targeted to the outer surface of the ER (19). This chimera, designated erPML, localized to the ER and MAMs in *Pml*$^{-/-}$ MEFs, as revealed by

immunocytochemical staining, immunogold labeling, and subfractionation (Fig. 3A and fig. S5). The introduction of erPML in *Pml*$^{-/-}$ MEFs restored $Ca^{2+}$ signals evoked by either agonist (Fig. 3B and fig. S6) or apoptotic stimuli (MEN or $H_2O_2$) (Fig. 3C) to values comparable to those in *Pml*$^{+/+}$ MEFs (Fig. 2, C and D). This effect was associated with a reestablished sensitivity to apoptosis induced by ER stress but did not restore the sensitivity to etoposide (ETO) (Fig. 3D and fig. S7A), a DNA-damaging agent that triggers apoptotic death by a $Ca^{2+}$-independent process (fig. S7B). Overall, these experiments indicate that the absence of Pml causes a reduction in the amplitude of $Ca^{2+}$ signals induced by ATP, other agents, or apoptotic stimuli, and that forcing PML to the ER rescues these defects. A PML protein targeted to the nucleus restored the formation of NBs, but did not restore the $Ca^{2+}$ responses and the sensitivity to ER stress–dependent cell death, although it restored response to other apoptotic stimuli such as ETO (fig. S8).

To investigate the mechanism underlying these activities of Pml, we tested whether Pml could functionally and physically interact with the $IP_3R3$. Immunoprecipitation of $IP_3R3$ led to the coprecipitation of Pml (Fig. 4A and fig. S9) and vice versa (fig. S10). Amounts of phosphorylated-$IP_3R3$ (p-$IP_3R3$) were higher in *Pml*$^{-/-}$ than in *Pml*$^{+/+}$ MEFs (Fig. 4A and fig. S11).

Reduced cellular sensitivity to apoptotic stimuli was observed in cells with high activity of the protein kinase Akt, as a result of diminished $Ca^{2+}$ flux from the ER through the $IP_3R$ (20,21). The amount of phosphorylated Akt (pAkt) (that is, the active form of Akt) coprecipitated with $IP_3R3$ (Fig. 4A and fig. S9) was higher in *Pml*$^{-/-}$ than in *Pml*$^{+/+}$ MEFs (fig. S11). Dephosphorylation of Akt at the MAM might occur through Pml-mediated recruitment of the phosphatase PP2a. Indeed, Pml interacts with PP2a in Pml-NBs (22). Further, the amount of PP2a coprecipitated with $IP_3R3$ (Fig. 4A and figs. S9 and S10) was diminished in *Pml*$^{-/-}$ MEFs (Fig. 4A and fig. S11). Thus, in the absence of *Pml*, reduced $Ca^{2+}$ release could be caused by increased phosphorylation and activation of Akt at the ER due to an impaired PP2a activity, which in turn impair $Ca^{2+}$ flux through the $IP_3R$ because of its hyperphosphorylated state (figs. S11 and S12).

To determine whether $IP_3R3$, Pml, Akt, and PP2a interact in a complex, we next performed two-dimensional blue native analysis. We found that Pml, $IP_3R3$, Akt, and PP2a colocalize in high molecular weight complexes, supporting their possible interaction in the native state (fig. S13). Finally, we demonstrated the localization of all these proteins at the ER and MAM through immunocytochemical staining and subfractionation (Fig. 4, B and C, and fig. S14).

We further investigated the correlation among Pml, Akt, and PP2a at the ER and the regulation of the $IP_3R$ by a selective inhibition of either Akt or PP2a. Pretreatment of cells with okadaic acid (OA, a PP2a inhibitor) caused a reduction in $[Ca^{2+}]_m$ responses to ATP stimulation and a reduced $H_2O_2$- or MEN-induced death in *Pml*$^{+/+}$ MEFs and in *Pml*$^{-/-}$ MEFs expressing erPML, but not in *Pml*$^{-/-}$ MEFs (Fig. 4, D and E, and figs. S15, S16, and S18), in which PP2a activity is impaired. LY294002 (an inhibitor of Akt) had no effect on the agonist-dependent $[Ca^{2+}]_m$ transients and on apoptosis in *Pml* $^{+/+}$ or *Pml* $^{-/-}$ MEFs expressing erPML, whereas it increased agonist-dependent $[Ca^{2+}]_m$ responses and restored sensitivity to $H_2O_2$ or MEN (Fig. 4, D and E, and figs. S15, S17, and S18) in *Pml*$^{-/-}$ MEFs (in which high levels of pAkt are observed; Fig. 4A and fig. S11). These results were confirmed in experiments in which RNA interference was used to deplete cells of Akt or PP2a proteins (fig. S19, A and B) or a constitutively active form of Akt (m/p Akt) was expressed (fig. S19C).

Our data highlight an extranuclear, transcription-independent function of Pml that regulates cell survival through changes in $Ca^{2+}$ signaling in the ER, cytosol, and mitochondria (fig. S20). This effect appears to be specific to $Ca^{2+}$-mediated apoptotic stimuli because alteration in Pml did not influence cell death in cells treated with ETO, which activates the apoptotic pathway in a way largely independent of $Ca^{2+}$.

This mechanism may explain how Pml can so broadly regulate the early (and transcription independent) apoptotic response. Our findings may have implications in tumorigenesis where the function of Pml is frequently lost, or in other patho-physiological conditions where Pml is accumulated such as cell stress, or infection with viral or bacterial pathogens.

## Supplementary Material

Refer to Web version on PubMed Central for supplementary material.

## References and Notes


1. Salomoni P, Pandolfi PP. Cell 2002;108:165. [PubMed: 11832207]
2. Gurrieri C, et al. J. Natl. Cancer Inst 2004;96:269. [PubMed: 14970276]
3. Shen TH, Lin HK, Scaglioni PP, Yung TM, Pandolfi PP. Mol. Cell 2006;24:331. [PubMed: 17081985]
4. Lin HK, Bergmann S, Pandolfi PP. Nature 2004;431:205. [PubMed: 15356634]
5. Condemine W, et al. Cancer Res 2006;66:6192. [PubMed: 16778193]
6. Bernardi R, Papa A, Pandolfi PP. Oncogene 2008;27:6299. [PubMed: 18931695]
7. Wieckowski MR, Giorgi C, Lebiedzinska M, Duszynski J, Pinton P. Nat. Protoc 2009;4:1582. [PubMed: 19816421]
8. Materials and methods are available as supporting material on *Science* Online.
9. Giorgi C, De Stefani D, Bononi A, Rizzuto R, Pinton P. Int. J. Biochem. Cell Biol 2009;41:1817. [PubMed: 19389485]
10. Pinton P, Giorgi C, Siviero R, Zecchini E, Rizzuto R. Oncogene 2008;27:6407. [PubMed: 18955969]
11. Hayashi T, Rizzuto R, Hajnoczky G, Su TP. Trends Cell Biol 2009;19:81. [PubMed: 19144519]
12. Patterson RL, Boehning D, Snyder SH. Annu. Rev. Biochem 2004;73:437. [PubMed: 15189149]
13. Giorgi C, Romagnoli A, Pinton P, Rizzuto R. Curr. Mol. Med 2008;8:119. [PubMed: 18336292]
14. Clapham DE. Cell 2007;131:1047. [PubMed: 18083096]
15. Pinton P, Rizzuto R. Cell Death Differ 2006;13:1409. [PubMed: 16729032]
16. Mendes CC, et al. J. Biol. Chem 2005;280:40892. [PubMed: 16192275]
17. Pinton P, Rimessi A, Romagnoli A, Prandini A, Rizzuto R. Methods Cell Biol 2007;80:297. [PubMed: 17445701]
18. Pinton P, et al. EMBO J 2001;20:2690. [PubMed: 11387204]
19. Yang M, Ellenberg J, Bonifacino JS, Weissman AM. J. Biol. Chem 1997;272:1970. [PubMed: 8999888]
20. Szado T, et al. Proc. Natl. Acad. Sci. U.S.A 2008;105:2427. [PubMed: 18250332]
21. Marchi S, et al. Biochem. Biophys. Res. Commun 2008;375:501. [PubMed: 18723000]
22. Trotman LC, et al. Nature 2006;441:523. [PubMed: 16680151]


23. This work was supported in part by grants from the National Cancer Institute (to P.P.P.); by K99 NIH (to I.K.); by AIRC, FISM, Telethon, Ministry of Health, and PRIN (to P.P.); by FP7 “MyoAGE”, NIH, Cariparo Foundation, and AIRC (to R. R.); and by grants from the Ministry of Science and Higher Education in Poland and the Polish Mitochondrial Network (to M.L., J.D., and M.R.W.). We thank S. Missiroli, F. Poletti, and C. Agnoletto for carrying out some experiments, and J. Meldolesi and members of the Pandolfi and Pinton lab for stimulating discussions.

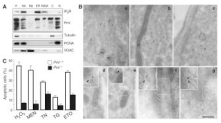

**Fig. 1.**

Identification of Pml at ER and MAM regions and $Ca^{2+}$-mediated Pml-dependent cell death. (**A**) Detection of Pml by immunoblotting in $Pml^{+/+}$ MEFs fractionation. $IP_3R$, tubulin, proliferating cell nuclear antigen (PCNA), and voltage-dependent anion channel (VDAC) are used as markers. H: homogenate; Mc: crude mitochondria; Mp: pure mitochondria; ER; MAM; C: cytosol; N: nucleus. (**B**) Immunogold labeling of Pml near the rough ER (r), mitochondria (m), and MAM (arrowheads) in $Pml^{+/+}$ MEFs. Gold particles (15 nm) are mostly associated with the surface of the ER (7.07 gold particles/$\mu m^2$) and more occasionally with mitochondrial membranes (3.08 gold particles/$\mu m^2$) (a and b). Specificity of the antibodies is demonstrated by labeling of nuclear bodies (n) (c). Morphologically identified MAM often demonstrated labeling at contacts between ER and mitochondria [(d) to (g), and arrowheads in insets therein]. Insets correspond to boxed areas. Bar: (a) 360 nm; (b) 340 nm; (c) 370 nm; (d) 188 nm, inset 120 nm; (e) 260 nm, inset 190 nm; (f) 340 nm, inset 180 nm; (g) 280 nm, inset 210 nm. (**C**) Apoptosis induced by 1 mM $H_2O_2$, 15 μM menadione (MEN), 6 μM tunicamycin (TN), 2 μM thapsigargin (TG), or 50 μM etoposide (ETO) in $Pml^{+/+}$ or $Pml^{-/-}$ MEFs treated for 12 hours. Data represent the mean SD of five independent experiments.

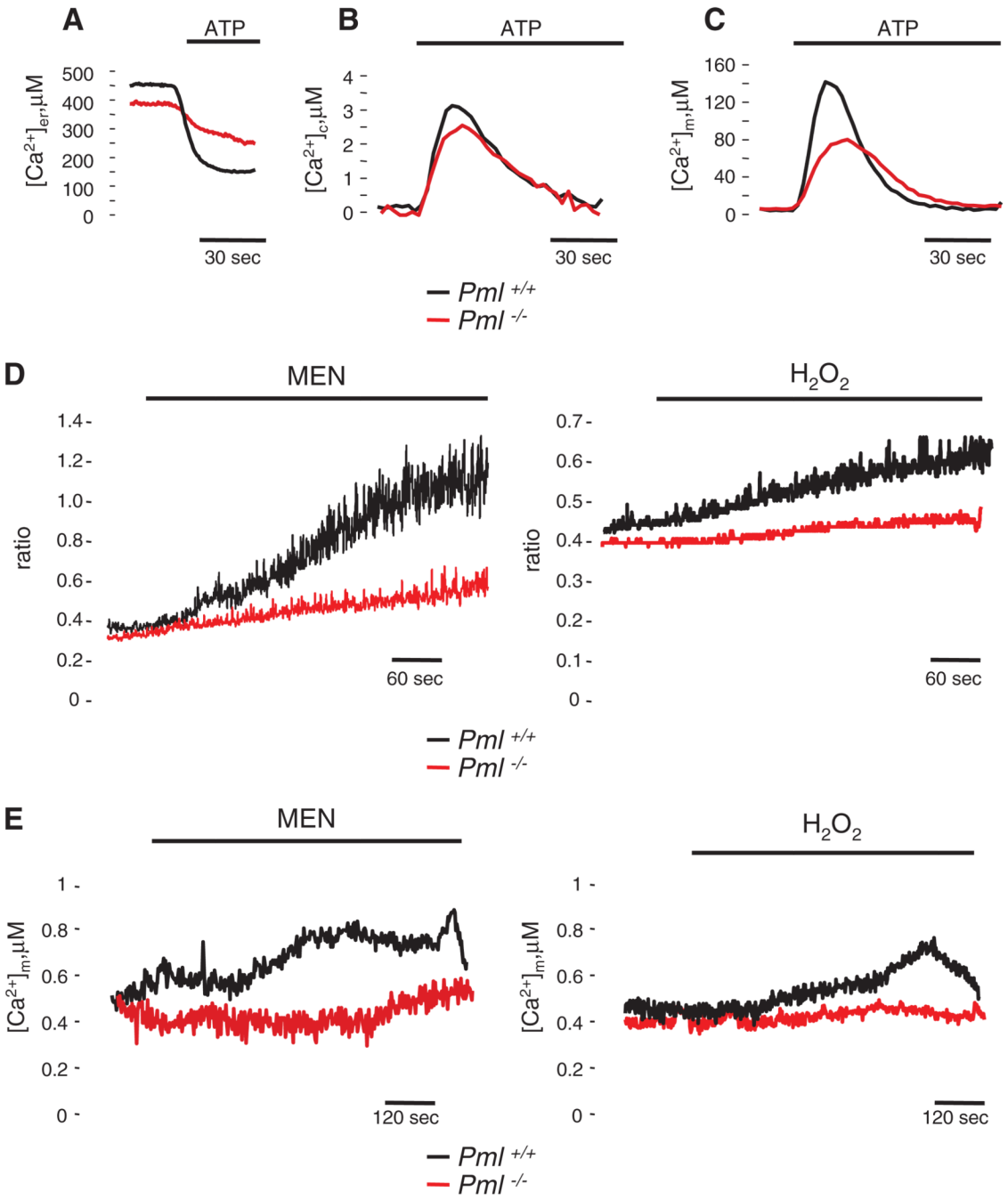


**Fig. 2.**

Intracellular $Ca^{2+}$ homeostasis in *Pml*$^{+/+}$ and *Pml*$^{-/-}$ MEFs. (**A** to **C**) ER (A), cytosolic (B), and mitochondrial (C) $Ca^{2+}$ homeostasis measurements with aequorins. Where indicated, cells were treated with 100 μM ATP. *Pml*$^{+/+}$: $[Ca^{2+}]_{ER}$ peak 448 ± 32 μM; $[Ca^{2+}]_c$ peak 3.3 ± 0.16 μM; $[Ca^{2+}]_m$ peak 138 ± 14 μM. *Pml*$^{-/-}$: $[Ca^{2+}]_{ER}$ peak 386 ± 42 μM; $[Ca^{2+}]_c$ peak 2.65 ± 0.23 μM; $[Ca^{2+}]_m$ peak 78 ± 10 μM. $n$ = 15 samples from five independent experiments, $P < 0.01$. (**D**) MEFs loaded with calcium-sensitive fluorescent dye fura-2 were stimulated with menadione (MEN) or $H_2O_2$. The kinetic behavior of the $[Ca^{2+}]_c$ response is presented as the ratio of fluorescence at 340 nm/380 nm. In these, and other fura-2 experiments, the traces are representative of at least 10 single-cell responses from three

independent experiments. (**E**) Analysis of $[Ca^{2+}]_m$ during oxidative stress. Where indicated, cells were stimulated with 30 μM MEN or 2 mM $H_2O_2$. *n* = 10 samples from three independent experiments.

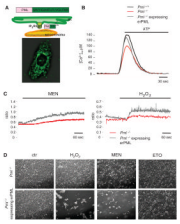

**Fig. 3.**

erPML chimera reestablishes the $[Ca^{2+}]_m$ and apoptotic responses in $Pml^{-/-}$ MEFs. (**A**) Schematic map of the erPML chimera and immunofluorescence image, stained with the antibody to PML, of $Pml^{-/-}$ MEFs expressing erPML. (**B**) erPML reestablishes the agonist-dependent $[Ca^{2+}]_m$ response in $Pml^{-/-}$ MEFs ($[Ca^{2+}]_m$ peak 135 ± 12 μM) to values comparable to those of $Pml^{+/+}$ MEFs. (**C**) $Pml^{-/-}$ and $Pml^{-/-}$ MEFs expressing erPML previously incubated with fura-2 were stimulated with menadione (MEN) or $H_2O_2$. (**D**) Representative microscopic fields of $Pml^{-/-}$ MEFs and $Pml^{-/-}$ expressing erPML before and after treatment with 1 mM $H_2O_2$, 15 μM MEN, or 50 μM etoposide (ETO) for 16 hours.

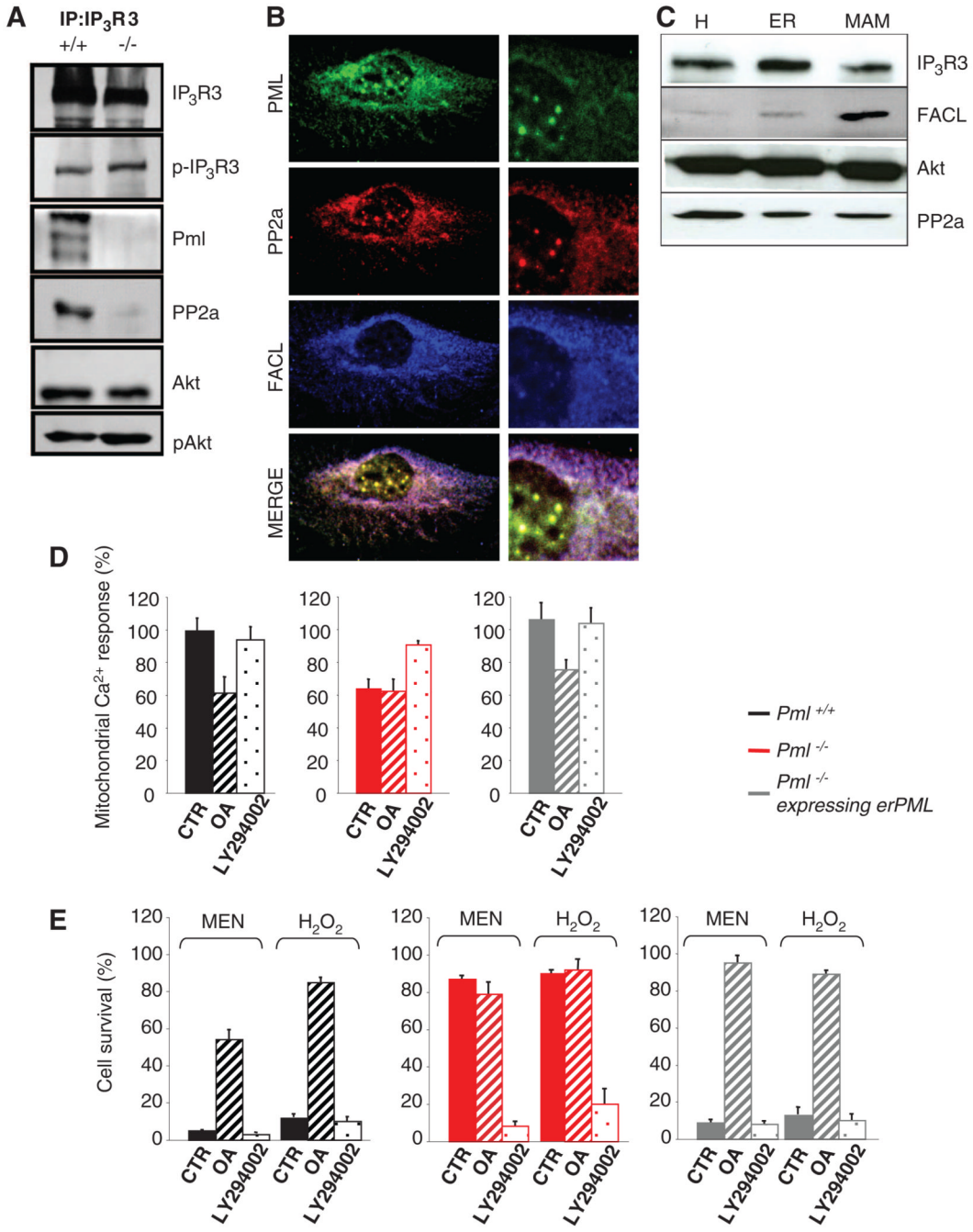


**Fig. 4.**

Modulation of $[Ca^{2+}]_m$ and apoptotic responses by Pml through Akt- and PP2a-dependent phosphorylation of $IP_3R3$. (**A**) Coimmunoprecipitation of $IP_3R3$ with Pml, Akt, and PP2a in $Pml^{+/+}$ MEFs. In the same blot, the levels of p-$IP_3R3$ and pAkt are shown. (**B**) Localization of Pml (green) and PP2a (red) at ER and MAM sites in $Pml^{+/+}$ MEFs analyzed by immunofluorescence. FACL [long-chain fatty acid–CoA (coenzyme A) ligase type 4, blue] was used as MAM marker. (**C**) $Pml^{+/+}$ MEFs subcellular fractionation and identification of PP2a and Akt at ER and MAM fractions by immunoblot. (**D**) Effects of okadaic acid (OA, 1 μM for 1 hour) and LY294002 (5 μM for 30 min) on agonist-dependent $[Ca^{2+}]_m$ responses in $Pml^{+/+}$, $Pml^{-/-}$, and $Pml^{-/-}$ MEFs expressing erPML. $[Ca^{2+}]_m$ is represented as a

percentage of the peak value of control cells. Representative traces are shown in fig. S15. (**E**) Quantification of cell survival of $Pml^{+/+}$, $Pml^{-/-}$, and $Pml^{-/-}$ MEFs expressing erPML, control (CTR, untreated) and treated first with OA (1 μM for 1 hour) or LY294002 (5 μM for 30 min) and then $H_2O_2$ or menadione (MEN) for 16 hours. The data show the percentage of living cells in the whole-cell population negative for annexin-V–fluorescein isothiocyanate and propidium iodide staining, analyzed by flow cytometry. Data show the means SD from three independent experiments.